

# Mammal remains at Rantis Cave, Israel, and Middle–Late Pleistocene human subsistence and ecology in the Southern Levant

JQS

OFER MARDER,<sup>1</sup> REUVEN YESHURUN,<sup>2\*</sup> RONIT LUPU,<sup>1</sup> GUY BAR-OZ,<sup>2</sup> MIRIAM BELMAKER,<sup>3</sup> NAOMI PORAT,<sup>4</sup> HAGAI RON<sup>5</sup> and AMOS FRUMKIN<sup>6</sup>

<sup>1</sup>Israel Antiquities Authority, POB 586, Jerusalem 91004, Israel

<sup>2</sup>Zinman Institute of Archaeology, University of Haifa, Mount Carmel, 31905 Haifa, Israel

<sup>3</sup>Department of Anthropology, Peabody Museum, Harvard University, USA

<sup>4</sup>Geological Survey of Israel, Jerusalem, Israel

<sup>5</sup>The Institute of Earth Sciences, Hebrew University, Jerusalem, Israel

<sup>6</sup>Department of Geography, Hebrew University, Jerusalem

Received 6 December 2009; Revised 16 January 2011; Accepted 14 February 2011

**ABSTRACT:** Rantis Cave is a recently discovered filled cave in central Israel, displaying a rich faunal accumulation of micro-mammals, ungulates and carnivores. U–Th dating assigns the beginning of accumulation to ca. 140 ka. The accumulation is culturally assigned to the late half of the Middle Paleolithic (MP) period. Single-grain optically stimulated luminescence measurements attest to a complex sedimentological history. We present the cross-disciplinary results of taphonomic and geomorphological analyses, which point to the cave serving as a natural pitfall trap for the large fauna, with little human or carnivore activity. The fauna is dominated by *Dama* among the ungulates and by *Microtus* among the micromammals. These data in conjunction with ungulate tooth mesowear analysis suggest a xeric Mediterranean environment on the eastern margin of the southern Levantine foothills. The relative taxonomic abundance of ungulate taxa shows some differences from anthropogenic MP sites, possibly reflecting the prey choice patterns of MP hunters. Overall, the natural accumulation scenario for Rantis Cave provides a rare paleoenvironmental and paleoeconomic reference to the rich anthropogenic MP faunas of the Southern Levant, enabling the reconstruction of a rich and diverse environmental setting for this important human dispersal route. Copyright © 2011 John Wiley & Sons, Ltd.

**KEYWORDS:** Levantine Middle Paleolithic; Middle–Late Pleistocene; paleoenvironments; taphonomy; zooarchaeology.

## Introduction

Several important archeological cave-sites dating to the Middle Paleolithic (MP), or to the late Middle Pleistocene – early Upper Pleistocene, are known in the Southern Levant (e.g. Tabun, Kebara, Skhul, Qafzeh, Hayonim, Amud and Misluya Caves). These sites normally contain thick human occupation layers with large quantities of lithics, anthropogenic features such as hearths and ash accumulations, and rich faunal assemblages, as well as early modern human and Neanderthal skeletal remains (e.g. Garrod and Bate, 1937; McCown and Keith, 1939; Neuville, 1951; Vandermeersch, 1981; Hovers *et al.*, 1995, 2000; Weinstein-Evron *et al.*, 2003; Bar-Yosef *et al.*, 2005; Bar-Yosef and Meignen, 2007). Fewer open-air sites are also known, usually representing much smaller accumulations of artifacts, animal bones and features left behind by MP humans (e.g. Rosh Ein Mor: Marks and Freidel, 1977; Far'ah II: Gilead and Grigson, 1984; Quneitra: Goren-Inbar, 1990; Ein Qashish: Hovers *et al.*, 2008; Nahal Mahanayem Outlet: Sharon *et al.*, 2010).

Most of the above-mentioned sites preserve rich faunal assemblages composed of large mammals and micromammals. The macrofaunal remains typically consist of carcasses acquired, processed and discarded by humans (e.g. Gilead and Grigson, 1984; Davis *et al.*, 1988; Rabinovich, 1990; Tchernov, 1992; Rabinovich and Tchernov, 1995; Rabinovich and Hovers, 2004; Stiner, 2005; Speth and Tchernov, 2007; Yeshurun *et al.*, 2007). These faunal remains have been used to infer hunting and subsistence patterns, as well as the paleoenvironments exploited by humans. Thus, large mammal-based paleoenvironmental reconstructions from the Levantine Pleistocene are derived from assemblages primarily formed by human activity, which are essentially human food

debris. The question of hunter prey choice and how it biases the fidelity of anthropogenic large mammalian assemblages is always pertinent in such contexts. Additionally, the micromammals found in MP sites have also played a pivotal role in the paleoenvironmental reconstructions of the MP (e.g. Tchernov, 1992, 1998).

Here we present the results of a multidisciplinary investigation of Rantis Cave in west-central Israel (Fig. 1). This recently discovered naturally filled cave yielded a rich faunal assemblage consisting primarily of micro- and macromammal remains with only meagre evidence for human occupation. Rantis Cave therefore allows for the exploration of Mid to Late Pleistocene paleoenvironments, associated with MP human activity, from a terrestrial accumulation that is primarily non-anthropogenic. Our aim is to shed light on the nature and timing of the faunal accumulation and to present it in the context of the rich zooarchaeological (anthropogenic) record from the region. The implications of our results for paleoenvironmental and paleoeconomic reconstructions in the Southern Levant during the Mid to Late Pleistocene are discussed.

## Regional setting

Rantis Cave is located at the western slopes of the Samaria Hills, within the western flanks of the Ramallah anticline, at an elevation of 220 m above sea level (map ref. NIG 200470–510/659240–282) (Fig. 1). The site lies in the Mediterranean phytogeographic zone of the Southern Levant (Danin, 1988), in an area of low limestone hills forming the transition from the coastal plain in the west to the Samaria highlands in the east. Today the region experiences a Mediterranean climate with rainy winters and dry summers. Mean annual precipitation is 600 mm, potential evaporation is 1600 mm and mean annual temperature is 19°C. Precipitation is mostly derived from western frontal systems, originating in the eastern Mediterranean.

\*Correspondence: R. Yeshurun, as above.  
E-mail: ryeshuru@research.haifa.ac.il

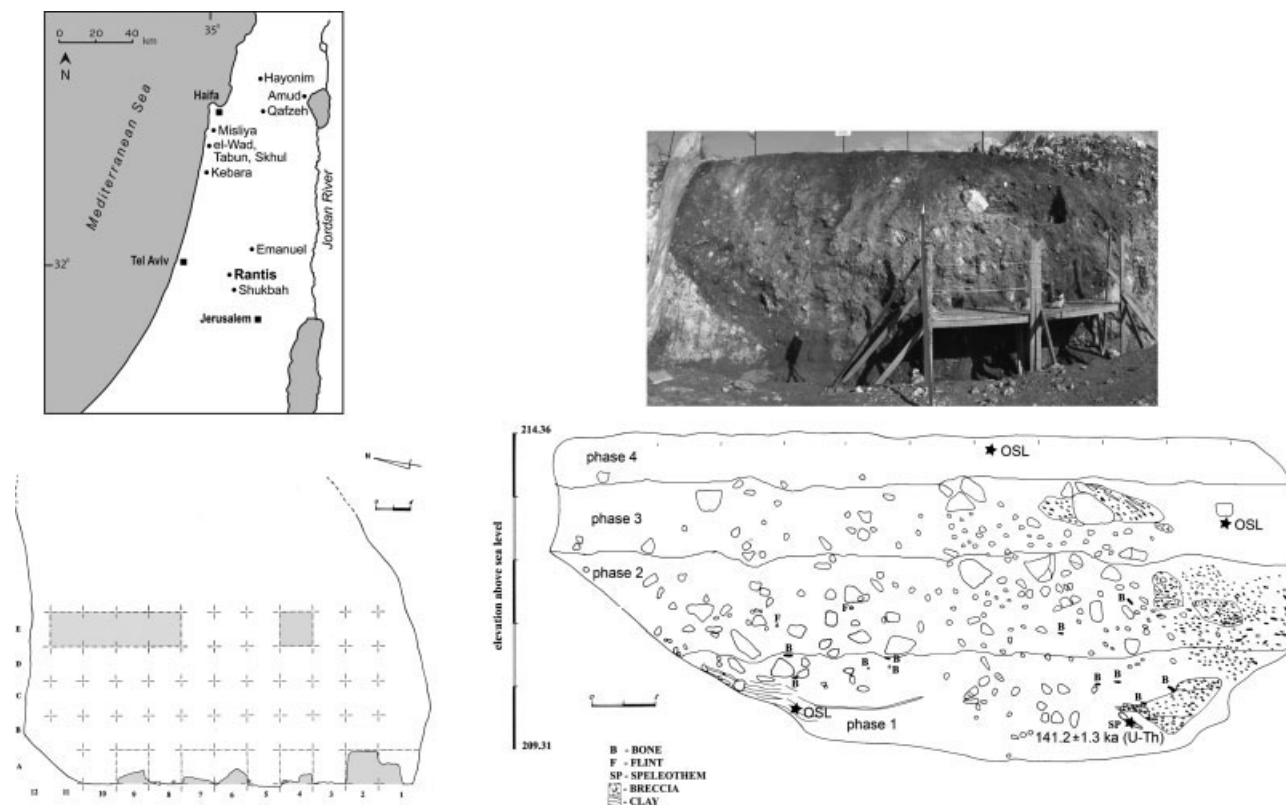


**Figure 1.** Rantis Cave: location map of the cave and other sites mentioned in the text; Plan of the excavation area by grid. Stratigraphic section and photograph looking east.

The site lies in the Bi'na Formation of Turonian age, which is the uppermost formation of the Judea Group, formed mostly in the shallow epicontinental southern Tethys Ocean (Sass and Bein, 1978) during the Late Cretaceous. The cave was formed within the massive, porous biosparitic limestone of the central member of the formation (Livnat, 1971). The bedrock dips gently south-westward. The Bi'na Formation is the richest in caves within the carbonate rocks of Israel, with over 1000 found in the mountain ridge forming the backbone of the country (Frumkin and Fischhendler, 2005; Frumkin and Gvirtzman, 2006; Frumkin *et al.*, 2009).

The Samaria, and in particular the Rantis region, are rich in isolated chamber caves, whose most common feature is a single chamber with phreatic morphology (Fischhendler and Frumkin, 2008). Karstification started during the late Turonian to early Santonian, when the area became locally uplifted above sea level. This is demonstrated by paleokarstic dolines filled with sand and Senonian marine sediments (Livnat, 1971). The Senonian transgression covered the entire area with chalk, which was later largely eroded except in some paleo-dolines as well as structural lows south of Rantis Cave. Regional uplift during the Mid to Late Cenozoic raised the region above sea level, promoting further karstification. Since the late Miocene the cave area has been subaerially exposed, promoting karst denudation. The Rantis Cave is a karstic isolated chamber, truncated by the abrasion-denudation terrace, and subsequently filled by sediments. Flowstone speleothems on the surface of the terrace above the cave indicate complete destruction of ancient caves during this process. There is no evidence of an underground stream, and the interfluvial location of the cave indicates that it has not been affected by surface streams during the Mid–Late Pleistocene.

Several other karstic caves containing Paleolithic sediments were recently discovered in this area as a result of construction activities: Qesem Cave displaying a long Acheulo-Yabrudian

sequence (Barkai *et al.*, 2003; Gopher *et al.*, 2005; Stiner *et al.*, 2009) and the MP Emanuel Cave (Peleg *et al.*, 2010). Additionally, the cave of Shukbah, excavated by Garrod (1942) in 1928 where MP and Natufian layers were revealed, is located just 6 km south-east of Rantis Cave.

## Site and excavation

The site was discovered in 2004 as a result of construction activities. A filled cave chamber, which comprised brown *terra rosa* soil with numerous animal bones and sporadic flint artifacts, was noticed in the section (Fig. 1). The cave is about 12 m wide (from north to south) and 5 m long (from east to west), which is small compared with the common size of chamber caves in the region (ranging from 10 to 50 m). The upper part of the cave underwent surface erosion. The depth from the present surface to the bottom is about 5 m; the eroded upper part of the cave was originally much higher. On the upper level, some traces of the cave outline can be seen (Fig. 1).

A salvage excavation was conducted at Rantis Cave on behalf of the Israel Antiquities Authority in 2005. Six 1-m<sup>2</sup> squares were excavated in the upper part of the cave surface (E-squares) and six squares on the lower part of the section (A-squares; Fig. 1). The squares were excavated in 10-cm spits and all the material was dry-sieved (2–5 mm mesh). One-fifth of the excavated sediments was wet-sieved through a 1-mm mesh.

## Stratigraphy

The Rantis Cave sequence shows an accumulation of fine-grain sediments combined with collapse debris of the cave roof and walls, with deposition of abundant faunal material and a few flint artifacts along the entire sequence. The cave fill was divided roughly into four stratigraphic phases, which reflect the series of events post-dating the opening of the cave ceiling. The

observed sedimentary sequence within the cave is described from bottom to top (Fig. 1).

### Phase 1

The lowermost part of the deposit (170 cm thick) is composed of *terra rosa* soil overlying the limestone bedrock. Within the *terra rosa* are thin layers of clays and concretions of manganese, preserved mainly at the northernmost lower part of the section (row A), suggesting waterlogged conditions. The sediments are occasionally cemented, appearing as lumps of breccia. Some isolated cobbles and boulders were found adjacent to the walls of the cave, as well as speleothem fragments. Two relatively well-preserved speleothem fragments were U–Th dated (see below).

### Phase 2

Phase 2 comprises partly brecciated pockets of *terra rosa* soil (150 cm thick) containing few flint artifacts and rich in animal bones, some of which underwent strong fossilization processes under wet conditions. They were deposited alongside residual blocks of karstified rocks in the center of the cave consisting of unsorted limestone boulders and cobbles.

### Phase 3

The upper part of the cave section (120 cm thick) consists of loose *terra rosa* soil, darker relative to the underlying phases, with small angular rock fragments and fewer cobbles and boulders.

### Phase 4

The uppermost part of the cave section (ca. 60 cm thick) is composed of dark gray *rendzina* that has been washed from the hillslopes, in part during the last millennia. Sediment samples from Phases 1, 3 and 4 were dated by optically stimulated luminescence (OSL; see below).

## Dating

We attempted to constrain the age of the Rantis Cave sequence by three different techniques: paleomagnetism, U–Th and OSL methods.

### Paleomagnetic measurements

Ten samples were taken for paleomagnetic measurements throughout the sequence. The soft soil material was sampled by carving a cubic pedestal, with a stainless steel knife, and then placing a non-magnetic plastic capsule over it. Orientation was determined with a Brunton compass before the sample was removed. Remnant magnetization of all samples was measured with a shielded three-axis superconducting 2G 750 SRM magnetometer with integrated alternating field coils at the paleomagnetic laboratory of the Hebrew University of Jerusalem. The natural remnant magnetization (NRM) was measured first, and then the specimens were subjected to stepwise demagnetization by alternating field with increasing intensity, from 5 to 80 mT, in 10-mT steps, which removed 90%

of the NRM intensity. The NRM intensity of all samples is  $10^{-2}$  A/m, which is four orders of magnitude stronger than the magnetization of the sample holder. The median destructive field is between 15 and 20 mT and a coercivity spectrum typical of cubic phase of probably magnetite or maghaemite composition. All samples show a stable northerly single vector declination and an upward (positive) moderate inclination as expected from axial dipole at 32°N latitude. The soil sequence of the Rantis Cave is therefore of normal magnetization and the age is younger than the Brunhes–Matuyama boundary, namely, younger than 780 ka (Baski *et al.*, 1992).

### U–Th dating

Two detached pieces of flowstone speleothems were found 0.5 m above the bottom of the cave, 2 m from the southern wall (Fig. 1). They are composed of laminar calcite, indicative of deposition by a slow-moving film of water and efficient CO<sub>2</sub> degassing across a large surface area (Ford and Williams, 2007). The flowstone was fragmented by erosion processes in the cave, and redeposited within its detrital fill. The well-preserved morphology indicates short transportation distance within the cave. The topmost, youngest layer of each speleothem (identified by its internal morphology) was U–Th dated (Table 1a) following the method described by Vaks *et al.* (2006, 2007).

Sample R-30 contains a small fraction of detrital thorium ( $^{230}\text{Th}/^{232}\text{Th} = 64.9$ ) and its age of  $141.2 \pm 1.3$  ka is the most accurate in this series. The second age,  $143.3 \pm 3$  ka (R-1A) (without correction), is less accurate due to high detrital thorium content ( $^{230}\text{Th}/^{232}\text{Th} = 6.3$ ). Because the two ages agree within errors, an age of  $\sim 140$  ka can be safely attributed to this flowstone.

### OSL dating

Three sediment samples were collected for OSL dating, from the base (Phase 1, sample RNS-41), middle (phase 3, sample RNS-44) and top (phase 4, sample RNS-43) of the section. This method dates the last exposure of mineral grains to sunlight, i.e. the time of deposition and burial (Aitken, 1998). In this carbonate rock terrain, the source of all the quartz is eolian, brought into the site by dust storms from a great distance, during which the grains are exposed to the sun and the OSL signal is reset. Only very fine sand-grade (74–125  $\mu\text{m}$ ) quartz was found in the samples, and it was extracted using routine laboratory procedures (Porat, 2007). Gamma and cosmic dose rates were measured in the field using a calibrated portable gamma counter. The beta and alpha dose rates were calculated from the concentrations of U, Th and K, measured from complementary sediment samples by ICP-MS. Mean water contents were estimated at  $10 \pm 3\%$ .

The conventional single aliquot regenerative dose protocol (Murray and Wintle, 2000) was first used to determine the equivalent dose ( $D_e$ ) on 2-mm aliquots. These preliminary measurements gave a large scatter on the  $D_e$  values (as much as 55%; Table 1b), probably as a result of complex cave-filling processes, when sediments that had accumulated at the surface

**Table 1a.** Dating results of speleothem samples from Rantis Cave

Sample	Age (ka)	+2 $\sigma$	−2 $\sigma$	$^{238}\text{U}$ (ppm)	[ $^{234}\text{U}/^{238}\text{U}$ ]	[ $^{230}\text{Th}/^{234}\text{U}$ ]	[ $^{230}\text{Th}/^{232}\text{Th}$ ]
R-30	141.2	1.3	1.3	2.259	$1.0535 \pm 0.0014$	$0.7336 \pm 0.0031$	64.89
R-1A	143.3	3.0	2.9	0.817	$1.005 \pm 0.002$	$0.7328 \pm 0.0071$	6.30

**Table 1b.** Luminescence results for conventional single aliquot measurements.

Sample	Location	Depth (m)	Field $\gamma$ ( $\mu\text{Gy a}^{-1}$ )	K (%)	U (p.p.m.)	Th (p.p.m.)	Ext. $\alpha$ ( $\mu\text{Gy a}^{-1}$ )	Ext. $\beta$ ( $\mu\text{Gy a}^{-1}$ )	Total dose ( $\mu\text{Gy a}^{-1}$ )	No. of discs	$D_e$ (Gy)	Age (ka)
RNS-41	Base of infill	4.0	575	0.33	3.1	4.7	11	670	1256 $\pm$ 59	6/6	324 $\pm$ 119	258 $\pm$ 95
RNS-44	Middle of infill	2.0	758	0.32	7.45	3.6	22	1157	1937 $\pm$ 87	11/14	406 $\pm$ 110	210 $\pm$ 57
RNS-43	Top of infill	0.6	794				$\sim$ 20	1129*	1943 $\pm$ 200	8/11	178 $\pm$ 97	92 $\pm$ 51

Measurements were carried out on 2-mm aliquots (200–300 grains). No. of discs = number of aliquots used for  $D_e$  calculations out of those measured. As chemical analyses were not available for sample RNS-43, the field-measured gamma + cosmic dose was used to estimate the beta dose. The ratio between the beta and gamma dose rates (without the cosmic component) of sample RNS-44 was used to estimate the beta dose rate of RNS-43. The large error on the dose rate (and hence the age) reflects the uncertainty.

were transferred into the cave with variable resetting of the OSL signal.

To isolate grains that could have been fully bleached at the time of deposition within the cave, single grains were measured, following the procedures outlined by Porat *et al.* (2006). Three-hundred single grains were measured for each sample, but due to the size of the holes on the measuring discs (300  $\mu\text{m}$ ) and the very fine sand-grade quartz, three or four grains filled each hole. Of the 300 measurements, 120–145 grains from each sample passed the quality assurance criteria (Table 1c). Most rejections were due to a saturated OSL signal, whereby laboratory irradiation could not regenerate the natural signal. The finite mixture model (Galbraith *et al.*, 1999) was used to separate the grains into age populations.

The single grain OSL measurements accentuated the scatter found within the conventional multiple grains  $D_e$  measurements, giving a very large range of ages within each sample (Table 1c). All samples contain a small population of very old grains with ages in the range 300–500 ka, but also a small population of young grains (17 to <17 ka), with the uppermost samples containing grains as young as 4 ka. The finite mixture model isolated 6–7 age populations within each sample and Table 1c gives the average, median and main population ages for each sample. About 36% of the grains in the sample from the base of the section (RNS-41) have an age range of 102–173 ka, but younger grains are very common. The most dominant population in the middle sample (RNS-44), comprising one-third of all grains, gave an age of 177  $\pm$  11 ka. The uppermost, youngest sample (RNS-43) contained very young grains (4–10 ka), and 18% of the grains are 26.1  $\pm$  2.8 ka, as expected from its position only 0.6 m below the surface, but also a substantial population (25%) with an age of 213  $\pm$  23 ka.

From the single grain results it is thus not possible to determine the exact timing of cave infill. Even the lowermost sample contains a few young grains, indicating that some mixing processes took place in the cave. The very old grains in all samples attest to a long history of sedimentary processes, whereby the sediment accumulated at the surface for a long time, only randomly being exposed to sunlight. At the time of

deposition little or no further exposure took place and probably sedimentation was rapid.

### Summary of dating

The stratigraphic setting of the flowstone indicates that most of the cave fill (from 0.5 m above the cave bottom upwards), as well as human and animal activities, post-dates  $\sim$ 140 ka. Due to the complex deposition processes, including recent pedogenesis at the upper layer, the attempted OSL dating was unable to provide a better chronologic resolution, even though a significant portion of the sediment grains correspond to the Th–U chronology.

### The lithic assemblage

The lithic assemblage consists of 39 flint artifacts, mostly unretouched flakes and chips made of gray-green, fine-grained, high-quality flint. Two oval-shaped, cobble-sized nodules were found in the excavation and it seems that a flint outcrop was located nearby, as flint nodules are embedded within the Bi'na formation (Sneh *et al.*, 1998). Although the sample is small (Lupu *et al.*, 2009) a detailed attribute analysis was conducted to define the lithic industry in the context of the Levantine Paleolithic (methods follow Goren-Inbar, 1990; Hovers, 2009).

The flakes ( $n = 24$ ) vary in size (length 20–61 mm, width 17–52 mm). The dorsal scar pattern is mostly simple along axis (Fig. 2: 4, 6, 8), although centripetal, ridged and bipolar patterns were also observed (Fig. 2: 2, 3, 7). Striking platforms are mostly plain (Fig. 2: 2, 3) or, less frequently, faceted (Fig. 2: 4, 5), cortical and relatively wide (Fig. 2: 8) (width 10–30 mm, thickness 3–18 mm). Core trimming elements included one oval/rounded débordant flake that was a rejuvenation flake of the Levallois production system (Fig. 2: 4). Only one core with a single striking platform was found; the preparation on its débitage surface resembles Levallois cores (Fig. 2: 1). A few tools ( $n = 7$ ) were retrieved, including notches, retouched flakes (Fig. 2: 5) and atypical transversal burin (Fig. 2: 7).

None of the artifacts is typologically diagnostic of a particular industry or period. However, the technological characteristics,

**Table 1c.** Single grain measurements results.

Sample	No. of grains	Average all grains (ka)	Median age (ka)	Component 1 (age ka)	Component 2 (age ka)	Component 3 (age ka)	Component 4 (age ka)
RNS-41	122/300	154 $\pm$ 146	97	38.1 $\pm$ 3.1 (15%)	63.6 $\pm$ 4.0 (24%)	102 $\pm$ 7 (20%)	173 $\pm$ 11 (16%)
RNS-44	143/300	296 $\pm$ 190	137	60.1 $\pm$ 4.2 (14%)	104 $\pm$ 7 (21%)	177 $\pm$ 11 (33%)	298 $\pm$ 18 (20%)
RNS-43	146/300	237 $\pm$ 214	79	26.1 $\pm$ 2.8 (18%)	51.5 $\pm$ 6.0 (19%)	109 $\pm$ 12 (17%)	213 $\pm$ 23 (25%)

No. of grains = number of grains selected for age calculations. Grains were selected if: (1) recycling ratios were within  $1 \pm 0.2$ ; (2) IR depletion ratios were less than 0.8; (3) error on  $D_e$  was less than 25%; (4) signal to background was  $> 3\sigma$ ; (5) laboratory dosing could reconstruct the natural signal (i.e. there is no signal saturation); and (6) the dose–response curve grew monotonously. The main components are shown with their respective percentage of the measured grains.

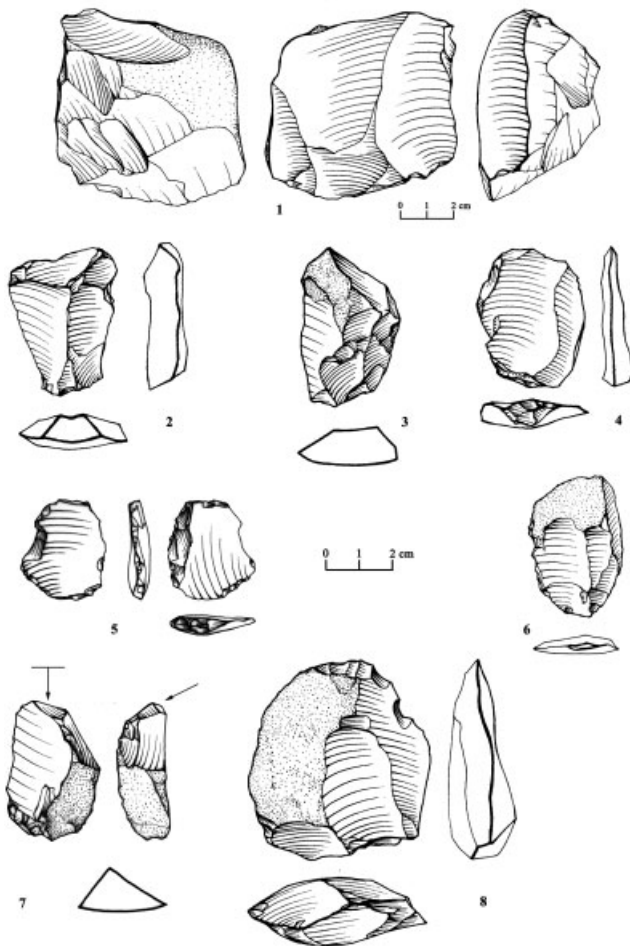


**Figure 2.** Flint artifacts from Rantis Cave.

such as plain or occasionally faceted platforms with a simple along axis-scar pattern, possibly imply that these flint artifacts were produced during the MP period, occasionally by the Levallois technique. The occurrence of one débordant flake and a presumably Levallois core underlines this observation.

## Faunal analysis

### Methods

Procedures of the faunal analysis followed Yeshurun *et al.* (2007). The bones were cleaned by immersing them in diluted acetic acid (5%) and subsequent buffering with KOH. When possible, bone fragments were identified to skeletal element and taxon (species or size-class) and were used to calculate the minimum number of elements (MNE; Lyman, 1994). The detailed identification and recording procedure was designed to achieve a maximum accuracy of the MNE count (see Marean *et al.*, 2004). All specimens identified were systematically examined for bone surface modifications, following the procedure described in Blumenschine *et al.* (1996; see Yeshurun *et al.* (2007) for a detailed account of the modifications recorded). As all samples accumulated under similar conditions and their taxonomic and taphonomic properties were very similar, the entire faunal assemblage was grouped together for the purpose of the following analyses.

The micromammal assemblage was collected by wet sieving of a sample of excavation units. The specimens were analysed under a stereoscopic microscope up to x60 magnification and identified to the lowest taxa possible. Recording of taphonomic variables (digestion, breakage patterns and abrasion) followed Andrews (1990).

An analysis of teeth mesowear, which measures attrition and abrasion on selenodont ungulate upper molars, was applied to suitable *Dama mesopotamica* teeth following the method described by Fortelius and Solounias (2000). Comparative results for modern taxa with known diets classified as browsers, grazers or mixed feeders were obtained from the literature (Fortelius and Solounias, 2000) as well as comparative samples from fossil *Dama* populations from Pleistocene South Levantine assemblages (Belmaker, 2008). This method was applied to assess the relative proportion of graze to browse in deer diet according to the proportion of graze in their environment (Hofman, 1989; Bodmer, 1990) and to use it as an additional paleoenvironmental proxy for the Rantis Cave fauna.

### The large mammal fauna

The bone assemblage of Rantis Cave is quite fragmented, although complete bone elements do occur. No articulated bones were identified during excavation. Despite our efforts, many of these fragments remained unidentified. The assemblage identified (number of identified specimens; NISP) is composed of 241 bone and tooth fragments, representing a minimum number (MNI) of 22 individual animals. The NISP and MNE values for every element in the fallow deer and gazelle size classes are presented in Supporting information, Table S1, and the bones identified to rarer species are detailed in supporting Table S2.

### Species representation and body size classes

Ungulate species (NISP = 228, including 130 fragments identified to size-class) dominate the assemblage, followed by carnivores (NISP = 11) and two hyrax (*Procavia* sp.) specimens. The most common species (Table 2) is Mesopotamian fallow deer (*Dama mesopotamica*, 68% of NISP). Other ungulates represented are mountain gazelle (*Gazella gazella*, 13%) and, to a lesser extent, aurochs (*Bos primigenius*), goat (*Capra* sp.) and wild boar (*Sus scrofa*). A similar representation was also found for specimens that were identified to size-classes corresponding to the three major ungulate species (i.e. Gazelle-size, Fallow deer-size and Aurochs-size). Species representation is similar among stratigraphic phases (Table 2).

**Table 2.** Large-mammal species representation at Rantis Cave.

	A Squares	E Squares	Total assemblage		
	NISP	NISP	NISP	%NISP	MNI
<i>Dama mesopotamica</i>	20	56	76	68	8
<i>Gazella gazella</i>	3	11	14	13	2
<i>Bos primigenius</i>	3	1	4	4	2
<i>Sus scrofa</i>	1	1	2	2	1
<i>Capra</i> sp.		3	3	3	2
<i>Panthera pardus</i>		4	4	4	1
<i>Canis lupus</i>	1	1	2	2	1
Small canid	2		2	2	1
<i>Ursus</i> sp.	1	1	2	2	1
<i>Hyena/Crocota</i>	1		1	1	1
<i>Procavia</i> sp.		2	2	2	1
Total ID to species	32	80	112	100	
<i>Dama</i> -size	24	85	109		
<i>Gazella</i> -size	8	10	18		
<i>Bos</i> -size	1	1	2		
Total ID	65	176	241		

Note: All identified elements (NISP), whether identified to species or to size-class, contributed to the MNE and MNI counts. MNI, minimum number of individuals, MNE, minimum number of elements.

The carnivore remains include five species: leopard (*Panthera pardus*, NISP = 4), wolf (*Canis lupus*, NISP = 2), brown bear (*Ursus arctos*, NISP = 2), a single undetermined species of hyena (*Hyena/Crocuta*) and a small canid, either fox (*Vulpes vulpes*) or jackal (*Canis aureus*) (Table 2; supporting Table S2). The bear species was identified as *Ursus arctos* on the basis of the breadth measurement of a lower  $M_2$  ( $B = 13.92$  mm), using Stiner *et al.*'s (1998) measurements for analogous teeth of *Ursus deningeri* and *Ursus arctos* as reference.

#### Ungulate mortality profiles

The age structure of the ungulate species was analysed on the basis of tooth eruption and wear, following Stiner's (1994, 2005) three-cohort age system (juvenile, prime and old). The fallow deer dental sample was the largest and the only one with a satisfactory, albeit small, sample size ( $n = 13$ ). The fallow deer exhibit a 'catastrophic' age profile, meaning that the juvenile age class is the largest, followed by prime-age adults and to a lesser extent by old adults (Fig. 3). This mortality profile is considered to conform closely to a natural age profile of a living population (Klein and Cruz-Urbe, 1984; Stiner, 1994).

#### Bone surface modifications

The bone cortical surfaces generally showed reasonable preservation, enabling us to search for various types of surface modifications. Human-induced butchery and consumption marks are nearly absent in the assemblage. Only a single burned specimen (a gazelle petrous bone) and one cut-marked specimen (a fallow deer mandible) were noted. None of the bones bears evidence of hammerstone percussion marks. Indications of animal modifications were also extremely rare in the assemblage, as no unambiguous carnivore gnaw marks were found, despite the systematic microscopic analysis, and only a single rodent gnaw mark was detected (Table 3).

Most bone surface modifications in the assemblage are the result of abiotic post-depositional agents (Table 3). Weathering damage is common (25% of the NISP were graded as stage 3 or higher, following Behrensmeyer's (1978) six weathering stages). This indicates that bones were exposed for a relatively long time. In addition, root marks appear on about one-third of the specimens. Lastly, five specimens show striations, caused either by trampling or by sediment compaction. Abrasion and rounding of bone edges, as well as bleaching, are infrequent, indicating that fluvial processes played a relatively minor role in the formation of the bone assemblages.

The bone surface modification data suggest that neither humans nor animals played an important role in the formation and modification of the Rantis Cave assemblage and that the bones were exposed to the elements and buried slowly. Similarly, processes such as fluvial transport do not seem to have modified the bone assemblage furthermore. It should be noted that little variation was found between the two

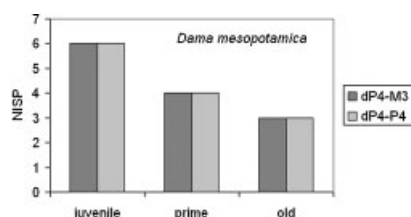


**Figure 3.** Mortality profile of Mesopotamian fallow deer in Rantis Cave, according to two possible dentition sequences (dP4-M3 and dP4-P4). NISP, number of identified specimens.

**Table 3.** Bone surface modification and fragmentation data from Rantis Cave.

	Gazelle size	Fallow deer size	Total*
NISP	32	185	217
Burned			
<i>n</i>	1	0	1
%	3	0	0
Green (V-shaped/spiral) fractures			
<i>n</i>	0	1	1
of	1	7	8
%	0	14	13
Shaft circumference (mm)			
<50	1	27	28
>50	0	1	1
100	4	5	9
Weathering ( $\geq$ stage 3)			
<i>n</i>	6	32	38
of	25	132	157
%	24	24	25
Cutmark			
<i>n</i>	0	1	1
%	0	1	1
Gnaw-mark (carnivore)			
<i>n</i>	0	0	0
%	0	0	0
Gnaw-mark (rodent)			
<i>n</i>	0	1	1
%	0	1	1
Root-mark			
<i>n</i>	10	44	54
%	40	33	35
Trampling striation			
<i>n</i>	0	5	5
%	0	4	3
Bleach			
<i>n</i>	1	3	4
%	4	2	3
Abrasion			
<i>n</i>	0	2	2
%	0	2	1

NISP, number of identified specimens. \*Bones identified to species and size-class combined.

excavation areas of the site, except for weathering damage, which is considerably higher in the A squares (the lower row).

#### Bone fracture patterns

Analysis of limb-bone fracture patterns followed Villa and Mahieu (1991) to determine the stage at which the bones were broken (i.e. fresh-green vs. old-dry). Although this analysis was based on a small sample of suitable specimens ( $n = 8$ ), it showed that most of the limb-bone fragmentation occurred post-depositionally. All but one specimen exhibited dry fractures resulting from non-nutritive breakage caused by trampling and/or sediment compaction of bones (Table 3). Most limb bone shafts in the Rantis Cave assemblage (74%) retained less than half of their original circumference (following Bunn, 1983), but a considerable portion of limb shafts (24%) still retained their full circumference (Table 3). This distribution of circumference types is similar to both anthropogenic and carnivore-den assemblages that were fully screened and collected (Marean *et al.*, 2004). Thus, the shaft circumference data do not yield further information about the accumulation agents of Rantis Cave, but it does demonstrate that the assemblage is not biased by collection methods and ensures the reliability of the observed skeletal-element profile (see below).

Comparison of bone fragment lengths between the two excavation areas showed them to be similar (Student's *t*-test,  $t = 0.58$ ,  $P = 0.56$ ), supporting the notion that bones in the two areas shared a similar taphonomic history.

#### Skeletal element frequencies

The skeletal element profile of fallow deer, the most abundant taxon at Rantis Cave, is heavily dominated by head parts, especially jaws, isolated teeth and the petrous bone (Fig. 4; bones identified to species and to size-class combined). This is also true for the small sample of gazelle bones (supporting Table S1). Limb bones, which are well represented in many of the MP sites of the Levant, are clearly under-represented at the cave assemblage, as are axial elements and toes. It is interesting to note that limb-bones with attached epiphysis outnumber shafts that lack an epiphysis (supporting Table S1), an uncommon characteristic among Pleistocene archaofaunas (Pickering *et al.*, 2003; cf. Yeshurun *et al.*, 2007: their Fig. 4).

It has been widely demonstrated that the survival of a skeletal element (i.e. its endurance to destruction agents) is mediated by its mineral density (Lyman, 1994). The relationship between the skeletal element survivorship of fallow deer (percentage of Minimum Animal Unit, %MAU) at Rantis Cave and bone mineral density (BMD<sub>1,2</sub> values for *Rangifer tarandus*; Lam *et al.*, 1999) shows a significant correlation (at the 0.1 level) between the two factors, which could account partially for the skeletal-element profile (Spearman's  $r = 0.26$ ,  $P = 0.07$ ; Fig. 5a). The fact that many intact jaws rather than isolated teeth, as well as some relatively weak elements such as limb epiphyses, ribs and vertebrae, are found in the assemblage may hint at rather moderate density-mediated destruction processes at the site. This could imply that the abundance of heads is not merely a taphonomic bias. The relationship between fallow deer skeletal element survivorship (%MAU; high-survival elements only) at Rantis Cave and its food utility index (FUI; Metcalfe and Jones, 1988) shows no correlation ( $r = -0.52$ ,  $P = 0.19$ ; Fig. 5b), indicating that meat-rich carcass parts were not selectively transported to the cave.

#### Micromammal remains

Microvertebrate remains derived from the site included numerous mammalia (a preliminary study of which will be presented below), amphibia, probably *Bufo* and *Rana*, as well as a large quantity of passerines and a few reptiles. Eight thousand fragments were retrieved from both area A and area E, of which ca. 10% were teeth identifiable to species. The list of species by MNI and NISP retrieved from the cave is presented in Table 4.

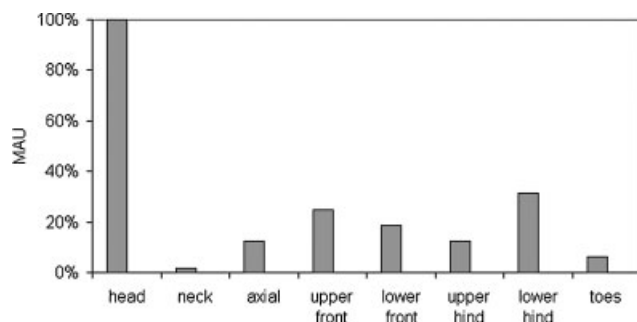


**Figure 4.** Skeletal-element frequency of the fallow deer at Rantis Cave (including elements identified to the fallow deer size class). Bone survivorship is demonstrated within eight anatomical zones (data from supporting Table S1; anatomical zones follow Stiner, 2002). MAU, Minimum Animal Unit.

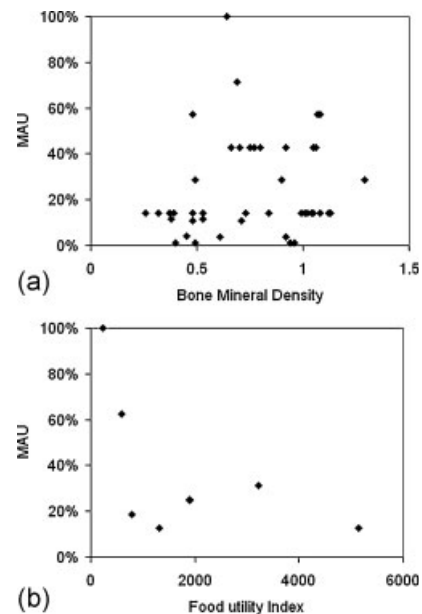


**Figure 5.** Relationship between fallow deer skeletal element survivorship (%MAU) at Rantis Cave and (a) bone mineral density (BMD<sub>1,2</sub> values for *Rangifer tarandus*; Lam *et al.*, 1999); and (b) food utility index (Metcalfe and Jones, 1988).

A detailed taphonomic account of the depositional history of the micromammal assemblage will be presented elsewhere. Here we note that the overall taphonomic imprints of both areas (A and E) are similar and suggest deposition by a raptor such as the barn owl (*Tyto alba*). There is low-level digestion on the salient edges of the microtine teeth (Andrews, 1990). However, post-depositional processes such as trampling and sediment compaction within the cave led to a highly fragmented assemblage, and thus there are no skulls and maxillae and very few limb elements with epiphyses were preserved. Moreover, mandibles lack rami and incisors, although molars are not loose. A growth of calcium carbonate crystals within the cavities of the micromammal bones (both teeth and post crania) points to chemical processes after the deposition of the bones.

The assemblages from the two excavated areas are very similar, as is the case based on the results of the lithic and large fauna analyses, which showed homogeneity throughout the site. In both areas, the overwhelming majority of the micromammal remains in the assemblage belong to the social vole *Microtus guenetheri* which accounts for ca. 85% of the assemblage. Other species, each accounting for up to 3% of the NISP and 10% of the MNI, include the house mouse (*Mus macedonicus*), Tristram's jird (*Meriones tristrami*), broad-tooth woodmouse *Apodemus sylvaticus*, Syrian squirrel (*Sciurus anomalus*) and shrew *Crocidura* spp.

The micromammal community of Rantis Cave is depauperate compared with other Mid-Late Pleistocene sites. Specifically, several Palearctic taxa which are common in the Galilee and Carmel sites such as Hayonim, Kebara and Amud Caves (Belmaker, in press) are absent or appear in very low abundances in the Rantis Cave micromammal communities. These include the hamsters (Cricetids) and the mouse-tailed dormouse (*Myomimus roachi*), which are absent, or several species of *Apodemus*, which are either absent or appear rarely in Rantis. However, Rantis Cave also lacks species indicative of an arid environment, such as the large shrew *Suncus murinus*, gerbils (*Gerbillus dasyrurus*) and the Arabian murids (*Mastomys batei* and *Arvicanthis ectos*). Their absence from Rantis Cave indicates that it was not situated in a semi-arid zone [as

**Table 4.** Composition of a studied sample of micromammal remains from Rantis Cave.

	Habitat	NISP (%NISP)		MNI (%)	
		A	E	A	E
<i>Microtus guentheri</i>	Grassland	1003 (96.7)	578 (93.1)	80 (89.88)	96 (84.95)
<i>Mus macedonicus</i>	Ubiquitous	9 (0.86)	24 (3.86)	4 (4.49)	12 (10.61)
<i>Meriones tristrami</i>	Grassland	21 (2.02)	13 (2.01)	2 (2.24)	1 (0.88)
<i>Apodemus cf. mastyacinus</i>	Woodland	1 (0.09)	4 (0.64)	1 (1.12)	2 (1.76)
<i>Crociodura</i> spp.	Ubiquitous	2 (0.2)	1 (0.16)	1 (1.12)	1 (0.88)
<i>Spalax ehernbergi</i>	Open habitats	1 (0.09)	0 (0)	1 (1.12)	0 (0)
<i>Sciurus anomalus</i>	Woodland	0 (0)	1 (0.16)	0 (0)	1 (0.88)
Total NISP		1037	621	89	113
Total fragments		ca. 11000	ca. 7000		

NISP, number of identified specimens; %NISP, percentage NISP.

suggested for MIS 5 of Qafzeh (Tchernov, 1998)] but within the Mediterranean zone, albeit a more xeric one.

### Mesowear analysis

The small fallow deer assemblage from Rantis Cave provided only nine complete upper molars amenable to mesowear analysis. Nonetheless, they provide valuable information regarding the paleoecology of the site. This sample consists of 100% high paracones, 66% sharps, 33.3% round and 0% blunt. To determine which diet conforms most to the Rantis Cave fallow deer mesowear results, a cluster analysis using standardized Euclidean amalgamation method was performed. A dendrogram is presented in Fig. 6. Two main clusters can be observed. The first includes taxa that are classified as grazers and as mixed feeders. The second includes browsers and mixed feeders. Modern fallow deer and most Levantine Pleistocene sites in the Galilee area (Tabun E, Kebara) are situated within this cluster and confirm modern observations that fallow deer are browsers. However, the Rantis Cave fallow deer population is situated within the cluster of grazers–mixed feeders. Although the Rantis Cave *Dama* included browse in their diet, it also had a high proportion of graze. This would suggest that the habitat around Rantis Cave was more open and xeric in comparison with the more northern regions.

### Discussion

Rantis Cave is a unique Pleistocene site in the Southern Levant, containing a rich faunal assemblage along with meager evidence for human occupation. The scanty anthropogenic evidence – a small lithic assemblage – hints at an occupation dated to the MP. The radiometric dates (U–Th) close to the bottom of the cave suggest that most deposition occurred after ca. 140 ka, culturally the late half of the MP. Sediments that accumulated on the surface over long periods prior to the cave opening were transferred into the cave pit by colluvial and gravitational mass movement, a process reflected in the OSL measurements.

The large-mammal assemblage of Rantis Cave is dominated by fallow deer and to a lesser extent by gazelle and other ungulates. It also includes very low frequencies of five different species of carnivores. The association between the ungulate remains, the carnivores and the few flint artifacts in the cave is not straightforward. The ungulate remains (mainly fallow deer) were probably not accumulated by humans (either hunters or scavengers), as they almost entirely lack signs of human butchery and consumption, in stark opposition to most other MP cave sites in the Levant (e.g. Rabinovich and Hovers, 2004; Stiner, 2005; Speth and Tchernov, 2007; Yeshurun *et al.*, 2007) or to the nearby late Lower Paleolithic Qesem Cave (Stiner

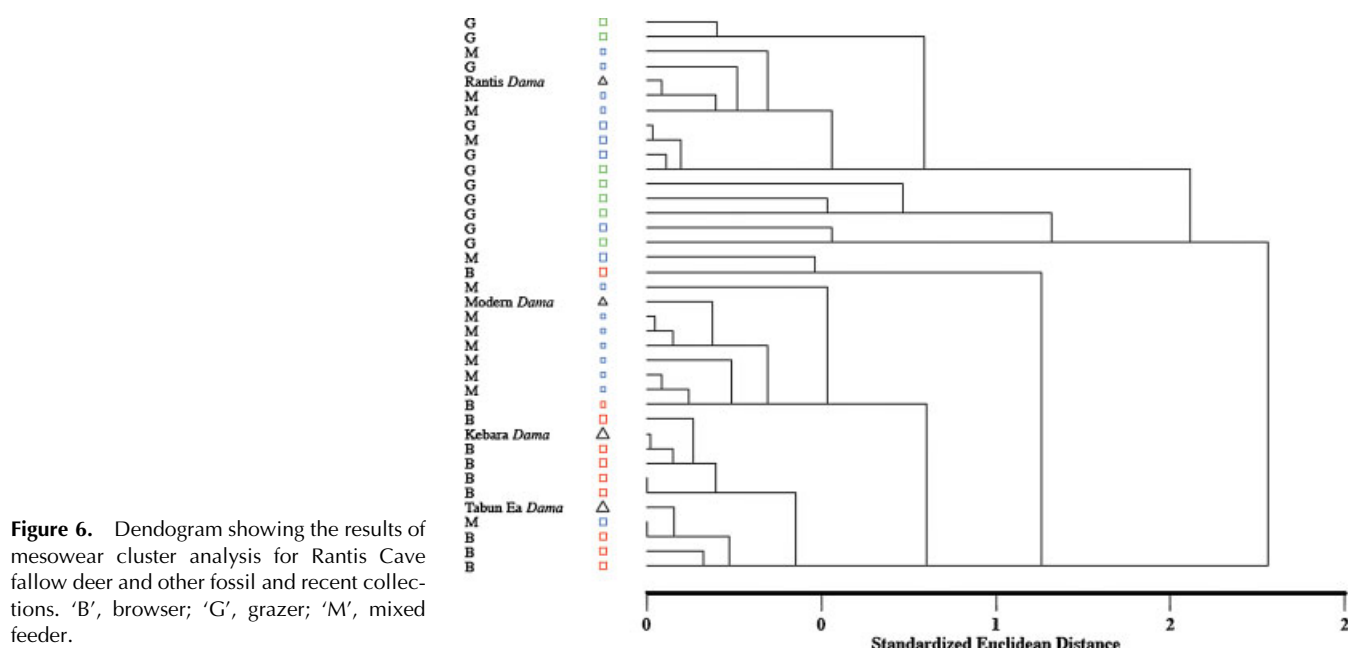


**Figure 6.** Dendrogram showing the results of mesowear cluster analysis for Rantis Cave fallow deer and other fossil and recent collections. 'B', browser; 'G', grazer; 'M', mixed feeder.



*et al.*, 2009). The juvenile-biased age distribution is unusual for a human hunting assemblage in this period (Stiner, 1994; Steele, 2005). Additionally, the head-dominated skeletal-element profile at the site is rare in faunas that were discarded by humans and have been fully analysed (Marean and Kim, 1998; Pickering *et al.*, 2003). It is notable that signs of fire are extremely rare in the site, again contrasting with other MP or Lower Paleolithic cave sites in the region (e.g. Karkanas *et al.*, 2007; Stiner *et al.*, 2011). Carnivores are not very abundant in the cave, carnivore-gnawed bones are absent and ungulate limb-bones with attached epiphysis outnumber shafts that lack an epiphysis – a pattern opposite to that expected in carnivore-ravaged assemblages (e.g. Marean and Spencer, 1991). Modern carnivore (hyena) dens in the region usually display some remains of large-carnivore pups, as well as small carnivore remains that served as prey to the larger carnivores, and many gnawed bones of a variety of taxa (e.g. Horwitz and Smith, 1988; Kuhn, 2005; see also Pickering, 2002; Rabinovich *et al.*, 2004; Kuhn *et al.*, 2010). However, this is not the situation at Rantis Cave. Thus, it appears that carnivores did not have an important effect on the ungulate assemblage and their visits to the site were sporadic and ephemeral.

Given the low anthropogenic impact at the site and on the faunal remains, the fact that the carnivore remains are few and scattered, the lack of signs for carnivore consumption and the 'catastrophic' age profile of the fallow deer, we suggest that the large mammal remains of Rantis Cave accumulated as a result of natural deaths either in the cave or in its immediate vicinity. Such 'natural death' sites are known globally, created either because of the existence of a pitfall trap or a by a catastrophic event (e.g. Shield Trap Cave: Oliver, 1989; Untermassfeld: Kahlke and Gaudzinski, 2005) but they are very rare in the Pleistocene of the Southern Levant (a notable exception is Bear's Cave in the Upper Galilee region of Israel: Tchernov and Tsoukala, 1997; see also Bunimovitz and Barkai, 1996). Humans and carnivores were intermittently attracted to the site, perhaps exploiting the dead ungulates (see below).

The taphonomic analysis and the geological investigations allow us to reconstruct the depositional history of Rantis Cave. A long period of karstification took place, first under the regional water table and then within the unsaturated zone. At this stage speleothems were actively growing under the roofed, wet cave conditions. The lowermost layers of clays and concretions of manganese, containing few faunal remains, could have been deposited at the bottom of the cave while it still had a roof or when a small opening in the roof just started to form. As a result of karst denudation the cave roof was widely opened and a doline-like structure was formed. An annual pond could have developed on the floor of the cave. At this stage animal carcasses started to accumulate inside. At the next stage more lateral parts of the doline collapsed, leaving residual blocks of karstified rocks in the center of the cave. Following the collapse, natural deaths of ungulates together with activity of predators and birds of prey occurred. Intense activity of nocturnal raptors in the immediate vicinity of the cave is evident by numerous micromammal remains. The single butchered bone specimen and several fresh flint artifacts indicate that short-term visits of humans to the cave area occurred at this stage, probably to exploit faunal resources (ungulate carcasses). This process continued until the upper part of the cave was sealed with dark gray *rendzina* that was washed from the hill slopes. At present, several chamber-shaped caves that probably went through the same processes are found in the vicinity of Rantis Cave; some were used as water holes in later periods (Fig. 7).

Several processes could explain the natural deaths of large mammals in Rantis Cave. The interfluvial location indicates that



**Figure 7.** A modern water hole in the vicinity of the cave – a possible reconstruction for the Rantis Cave pitfall.

it has not been significantly affected by surface streams, so animal remains could hardly be washed into the cave. This is supported by the fresh, unabraded condition of the artifacts and bones. However, some water probably accumulated within the doline. Animals must have been attracted to water, and could then be trapped in the sinkhole, with the vertical and overhanging walls offering no escape route. The probable standing water and the geometry of the sinkhole probably ruled out occupation by non-flying animals and by humans. Thus, we suggest that Rantis Cave acted as a natural pitfall that trapped the animals inhabiting the landscape.

The Mesopotamian fallow deer, the dominant large mammal at the cave, has been considered to represent woodland environment since the first paleoenvironmental reconstructions of the Levant (Bate, 1937; see also Garrard, 1982; Mendelssohn and Yom-Tov, 1999). It is very common in other Levantine Pleistocene faunas (e.g. Davis, 1977; Tchernov, 1992), but at present it is extremely rare in the wild (Chapman and Chapman, 1997). The ongoing reintroduction of this species to Israel (Saltz, 1998) has provided some new data on its ecology and behavior. Observations on the reintroduced herd showed that the animals prefer a moderate terrain and dense Mediterranean woodland rather than scrubland or open pastures (although the latter is also important for feeding). Interestingly, one fawn was found dead in a water hole into which it presumably fell (Bar-David *et al.*, 2005a, b). These data support the notion that the abundance of fallow deer remains at Rantis Cave signals a woodland environment and may support our notion as to the possibility of the cave acting as a pitfall.

The probable existence of a naturally accumulated large-mammal assemblage at Rantis Cave indicates that the macrofaunal remains may be used for paleoenvironmental inferences, independently of human prey choices. The prevalence of *Dama mesopotamica* would point to dense oak woodland environment on the western flanks of the Samaria hills during Marine Isotope Stage (MIS) 6a and later. However, a preliminary multivariate analysis with the micromammal remains and the mesowear data suggests a more complex picture.

The micromammals of the cave were deposited as a result of predation by owls. The assemblage is highly dominated by the social vole, which inhabits open fields, seemingly in contrast to the abundance of fallow deer which inhabit dense woodlands. The high proportions of microtines may be due to taphonomic bias caused by barn owl predation (Yom-Tov and Wool, 1997; Torre *et al.*, 2004; Reed, 2005). Yet even when microtines are

excluded from the analysis, the non-microtine taxonomic composition of Rantis Cave includes fewer woodland taxa than most sites in the Mediterranean zone of northern Israel, such as Hayonim E, Kebara F and Tabun C, and is thus suggestive of a more xeric environment. Nonetheless, it is worth noting that both the broad-tooth wood mouse and the Syrian squirrel are present, albeit in low numbers, suggesting that some woodland was present in the region. The mesowear analysis suggests a fallow deer diet which is higher in graze relative to both modern populations and other MP fossil populations, supporting the reconstruction of a more xeric environment as suggested by the micromammal analysis. Taken together, the analyses of the Rantis Cave fauna suggest that the cave was situated in the xeric Mediterranean region and included sparser woodlands compared with the Mount Carmel and Galilee regions further north.

The MP of the Levant, occupying MIS7 to the beginning of MIS3 (ca. 240–50 ka), is usually manifested by densely occupied cave sites preserving huge amounts of cultural remains, or by smaller open-air sites that also document human habitation events. Rantis Cave shows only meager evidence for human presence, in the form of a few lithic artifacts and one butchered bone. The cave was probably an opportunistic station in the foraging area of MP human groups, for consuming fresh ungulate carcasses deposited in the chamber, but was not used for human habitation. It is possible that most of the similar sites exploited sporadically by MP human groups have low archaeological visibility, if they survived at all; Rantis Cave therefore offers a unique (albeit meager) testimony to the activities undertaken by MP humans outside of their repeatedly occupied habitation sites.

In contrast to most other MP sites in the region, the large-mammal assemblage of Rantis Cave is largely unbiased by human predation. Nonetheless, it shows remarkable similarity in the presence of mammal species with the human-predated assemblages found at other MP sites, comprising primarily *Dama*, *Gazella*, *Bos*, *Sus* and *Capra*. These results support the notion that MP human foragers mostly hunted the ungulate taxa that were present in the landscape (see Bar-Yosef, 2004) so that human prey choices largely reflected taxa availability. However, Rantis Cave displays a higher percentage of fallow deer than most MP faunal assemblages in the Mediterranean Southern Levant, where the frequencies of mountain gazelles are significant (e.g. Davis, 1977; Garrard, 1982; Rabinovich and Hovers, 2004; Stiner, 2005; Speth and Tchernov, 2007; Yeshurun *et al.*, 2007). This may indicate a hunting preference for gazelles in some of the contemporaneous sites, continuing into later periods (e.g. Davis *et al.*, 1988; Rabinovich, 2003; Bar-Oz, 2004; Yeshurun, 2010).

## Summary and conclusions

The recently discovered Rantis Cave displays an accumulation culturally within the late half of the MP. Taphonomic and geological analyses point to a natural pitfall trap with little human or carnivore activity. Large faunal remains are dominated by fallow deer while micromammal remains are dominated by the social vole. The paleoecological reconstruction largely indicates a xeric Mediterranean environment on the eastern margin of the Southern Levantine coastal plain. Our faunal-based reconstruction indicates a rich and diverse environmental setting for this important human dispersal route (Frumkin *et al.*, 2011). The ungulate and carnivore taxa present in this natural accumulation are the same as known from contemporaneous anthropogenic sites, but the abundance of fallow deer at Rantis Cave is higher than at most anthropogenic sites. This indicates that MP humans hunted the game available

in their vicinity, but with some prey-choice patterns that are possibly reflected in the faunas preserved in their habitation sites. Overall, the unique accumulation scenario for Rantis Cave provides a rare comparison with the anthropogenic MP sites in the Mediterranean zone of the Levant and allows us to evaluate hypotheses regarding faunal-based paleoecological reconstructions and hunter choice in this period.

## Supporting information

Additional supporting information can be found in the online version of this article:

Table S1 NISP and MNE values for each bone portion in the two major size classes in the Rantis Cave assemblage.

Table S2 Bones of rare species recorded in the Rantis Cave assemblage.

Please note: As a service to our authors and readers, this journal provides supporting information supplied by the authors. Such materials are peer-reviewed, and may be re-organized for online delivery, but are not copy-edited or typeset by Wiley-Blackwell. Technical support issues arising from supporting information (other than missing files) should be addressed to the authors.

**Acknowledgements.** We thank N. Goren-Inbar, E. Hovers, N. Marom, G. Sharon, M. Weinstein-Evron, L. Weissbrod and two anonymous reviewers for commenting on earlier drafts of the manuscript. The Rantis Cave excavation was undertaken on behalf of the Israel Antiquities Authority and financed by the Israel Ministry of Defense. M.B. is funded by the American School of Prehistoric Research (ASPR), Harvard University, and wishes to thank J. Chupasko for access to the Mammalian Collections at the Museum of Comparative Zoology, Cambridge, MA. We would like to thank students and colleagues for their assistance in the field and analysis, especially R. Rabinovich, A. Barash, O. Ackermann, A. Belfer-Cohen and N. Goring-Morris. The flint artifacts were illustrated by L. Zeiger. The U–Th and OSL analyses were carried out at the Geological Survey of Israel.

**Abbreviations.**  $D_e$ , equivalent dose; MAU, Minimum Animal Unit; MIS, Marine Isotope Stage; MNE, minimum number of elements; MNI, minimum number of individuals; MP, Middle Paleolithic; NISP, number of identified specimens; NRM, natural remnant magnetization; OSL, optically stimulated luminescence.

## References

- Aitken MJ. 1998. *An Introduction to Optical Dating*. Oxford University Press: Oxford.
- Andrews P. 1990. *Owls, Caves and Fossils*. University of Chicago Press: Chicago.
- Bar-David S, Saltz D, Dayan T. 2005a. Predicting the spatial dynamics of a reintroduced population: the Persian fallow deer. *Ecological Applications* **15**: 1833–1846.
- Bar-David S, Saltz D, Dayan T, *et al.* 2005b. Demographic models and reality in reintroductions: the Persian fallow deer in Israel. *Conservation Biology* **19**: 131–138.
- Barkai R, Gopher A, Lauritzen SE, *et al.* 2003. Uranium series dates from Qesem Cave, Israel, and the end of the Lower Palaeolithic. *Nature* **423**: 977–979.
- Bar-Oz G. 2004. *Epipaleolithic Subsistence Strategies in the Levant. A Zooarchaeological Perspective*. ASPR Monograph Series. Brill: Boston.
- Bar-Yosef O. 2004. Eat what is there: hunting and gathering in the world of Neanderthals and their neighbors. *International Journal of Osteoarchaeology* **14**: 333–342.
- Bar-Yosef O, Meignen L. 2007. (eds). *Kebara Cave, Mt. Carmel, Israel. The Middle and Upper Palaeolithic Archaeology*. Part 1. Peabody Museum of Archaeology and Ethnology: Cambridge MA.
- Bar-Yosef O, Belfer-Cohen A, Goldberg P, *et al.* 2005. Archaeological background to Hayonim Cave and Meged Rockshelter. In *The Faunas of Hayonim Cave (Israel): A 200,000-Year Record of Paleolithic Diet*,

- Demography and Society*, Stiner MC (ed.). Peabody Museum of Archaeology and Ethnology: Cambridge, MA; 17–38.
- Baski A, Hsu V, McWilliams M, et al. 1992. Dating of the Brunhes-Matuyama geomagnetic reversal. *Science* **256**: 356–357.
- Bate DMA. 1937. Palaeontology: the fossil fauna of the Wadi el-Mughara Caves. In *The Stone Age of Mount Carmel, Excavations at the Wadi Mughara*, vol. I, Garrod DAE, Bate DMA (eds). Clarendon Press: Oxford; 135–240.
- Behrensmeyer AK. 1978. Taphonomic and ecological information from bone weathering. *Paleobiology* **4**: 150–162.
- Belmaker M. 2008. Paleodietary analysis of medium-sized cervids in 'Ubeidiya, Israel: evidence for Mediterranean oak woodland habitat in the Early Pleistocene of the Jordan Valley and its bearing on climatic hypotheses of 'Out of Africa I'. *PaleoAnthropology* **2008**: A3.
- Belmaker M. in press. The Southern Levant during the Last Glacial and zooarchaeological evidence for the effects of climatic-forcing on hominin population dynamics. In *Climate Change, Human Response and Zooarchaeology*, Monks G (ed). Vertebrate Paleobiology and Paleoanthropology Series. Springer: Dordrecht.
- Blumenschine RG, Marean CW, Capaldo SD. 1996. Blind tests of inter-analyst correspondence and accuracy in the identification of cut marks, percussion marks, and carnivore tooth marks on bone surfaces. *Journal of Archaeological Science* **23**: 493–507.
- Bodmer RE. 1990. Ungulate frugivores and the browser-grazer continuum. *Oikos* **57**: 319–325.
- Bunimovitz S, Barkai R. 1996. Ancient bones and modern myths: Ninth millennium BC hippopotamus hunters at Akrotiri Aetokremnos, Cyprus? *Journal of Mediterranean Archaeology* **9**: 83–94.
- Bunn HT. 1983. Evidence on the diet and subsistence patterns of Plio-Pleistocene hominids at Koobi Fora, Kenya, and Olduvai Gorge, Tanzania. In *Animals and Archaeology 1: Hunters and Their Prey*, Clutton-Brock J, Grigson C (eds). British Archaeological Report: Oxford; 21–30.
- Chapman DI, Chapman NG. 1997. *Fallow Deer: Their History, Distribution and Biology*, 2nd edn. Coch-y-bonddu books: Machynlleth, Powys, UK.
- Danin A. 1988. Flora and vegetation of Israel and adjacent areas. In *The Zoogeography of Israel*, Yom Tov Y, Tchernov E (eds). Dr. W. Junk Publishers: Dordrecht; 129–159.
- Davis S. 1977. The ungulate remains from Kebara Cave. *Eretz-Israel* **13**: 150–163.
- Davis SJM, Rabinovich R, Goren-Inbar N. 1988. Quaternary extinctions and population increase in Western Asia: the animal remains from Biq'at Quneitra. *Paléorient* **14**: 95–105.
- Fischhendler I, Frumkin A. 2008. Distribution, evolution and morphology of caves in south-western Samaria, Israel. *Israel Journal of Earth Sciences* **57**: 311–322.
- Ford DC, Williams PW. 2007. *Karst Hydrogeology and Geomorphology*. Wiley: Chichester.
- Fortelius M, Solounias N. 2000. Functional characterization of ungulate molars using the abrasion - attrition wear gradient: a new method for reconstructing paleodiets. *American Museum Novitates* **3301**: 1–36.
- Frumkin A, Fischhendler I. 2005. Morphometry and distribution of isolated caves as a guide for phreatic and confined paleohydrological conditions. *Geomorphology* **67**: 457–471.
- Frumkin A, Gvirtzman H. 2006. Cross-formational rising groundwater at an artesian karstic basin: the Ayalon Saline Anomaly, Israel. *Journal of Hydrology* **318**: 216–333.
- Frumkin A, Karkanas P, Bar-Matthews M, et al. 2009. Gravitational deformations and fillings of aging caves: the example of Qesem karst system, Israel. *Geomorphology* **106**: 154–164.
- Frumkin A, Bar-Yosef O, Schwarcz HP. 2011. Possible paleohydrologic and paleoclimatic effects on hominin migration and occupation of the Levantine Middle Paleolithic. *Journal of Human Evolution* in press.
- Galbraith RF, Roberts RG, Laslett GM, et al. 1999. Optical dating of single and multiple grains of quartz from Jinmium rock shelter, northern Australia: Part I. Experimental design and statistical models. *Archaeometry* **41**: 339–364.
- Garrard AN. 1982. The environmental implications of the re-analysis of the large mammal fauna from the Wadi el-Mughara Caves, Palestine. In *Paleoclimates, Paleoenvironments and Human Communities in the Eastern Mediterranean Region in Later Prehistory*, Bintliff JL, Van Zeist W (eds). BAR International Series: Oxford; 165–198.
- Garrod DAE. 1942. Excavations at the cave of Shukbah (Palestine). *Proceedings of the Prehistoric Society* **8**: 1–20.
- Garrod DAE, Bate DMA. 1937. *The Stone Age of Mount Carmel. Excavations at the Wadi Mughara*, vol. I. Clarendon Press: Oxford.
- Gilead I, Grigson C. 1984. Farah II: a Middle Paleolithic open-air site in the Northern Negev, Israel. *Proceedings of the Prehistoric Society* **50**: 71–97.
- Gopher A, Barkai R, Shimelmitz R, et al. 2005. Qesem Cave: an Amudian site in Central Israel. *Journal of the Israel Prehistoric Society* **35**: 69–92.
- Goren-Inbar N. 1990. *Quneitra: A Mousterian Site on the Golan Heights*. Qedem Monographs of Archaeology: Jerusalem.
- Hofman R. 1989. Evolutionary steps of ecophysiological adaptation and diversification of ruminants: a comparative view of their digestive system. *Oecologia* **78**: 443–457.
- Horwitz LK, Smith P. 1988. The effect of striped hyena activity on human remains. *Journal of Archaeological Science* **15**: 471–481.
- Hovers E. 2009. *The Lithic Assemblages of Qafzeh Cave*. Oxford University Press: New York.
- Hovers E, Buller A, Ekshtain R, et al. 2008. 'Ein Qashish - A New Middle Paleolithic open-air site in northern Israel. *Journal of the Israel Prehistoric Society* **38**: 7–40.
- Hovers E, Kimbel WH, Rak Y. 2000. The Amud 7 skeleton – still a burial. Response to Gargett. *Journal of Human Evolution* **39**: 253–260.
- Hovers E, Rak Y, Lavi R, et al. 1995. Hominid remains from Amud Cave in the context of the Levantine Middle Palaeolithic. *Paléorient* **21**: 47–61.
- Kahlke R-D, Gaudzinsky S. 2005. The blessing of a great flood: differentiation of mortality patterns in the large mammal record of the Lower Pleistocene fluvial site of Untermassfeld (Germany) and its relevance for the interpretation of faunal assemblages from archaeological sites. *Journal of Archaeological Science* **32**: 1202–1222.
- Karkanas P, Shahack-Gross R, Ayalon A, et al. 2007. Evidence for habitual use of fire at the end of the Lower Paleolithic: Site-formation processes at Qesem Cave, Israel. *Journal of Human Evolution* **53**: 197–212.
- Klein RG, Cruz-Urbe K. 1984. *The Analysis of Animal Bones from Archaeological Sites*. University of Chicago Press: Chicago.
- Kuhn B. 2005. The faunal assemblages and taphonomic signatures of five striped hyenas (*Hyena hyena sryaca*) dens in the desert of Eastern Jordan. *Levant* **37**: 221–234.
- Kuhn F, Berger LR, Skinner JD. 2010. Examining criteria for identifying and differentiating fossil faunal assemblages accumulated by hyenas and hominins using extant hyenid accumulations. *International Journal of Osteoarchaeology* **20**: 15–35.
- Lam YM, Chen X, Pearson OM. 1999. Intertaxonomic variability in patterns of bone density and the differential representation of bovid, cervid and equid elements in the archaeological record. *American Antiquity* **64**: 343–362.
- Livnat A. 1971. *The geology of the north-western foothills of Judean Mountains (Abud-Qibya-Rantis region)*. MA thesis, The Hebrew University, Jerusalem (in Hebrew).
- Lupu R, Marder O, Frumkin A, et al. 2009. Rantis Cave. *Excavations and Surveys in Israel* 121 (available at [http://www.hadashot-esi.org.il/report\\_detail\\_eng.asp?id=1165&mag\\_id=115&previewit=TrUe](http://www.hadashot-esi.org.il/report_detail_eng.asp?id=1165&mag_id=115&previewit=TrUe)).
- Lyman RL. 1994. *Vertebrate Taphonomy*. Cambridge University Press: Cambridge.
- Marean CW, Dominguez-Rodrigo M, Pickering TR. 2004. Skeletal element equifinality in zooarchaeology begins with method: the evolution and status of the "Shaft Critique". *Journal of Taphonomy* **2**: 69–98.
- Marean CW, Kim SY. 1998. Mousterian large mammal remains from Kobeh Cave: behavioral implications for Neandertals and Early Modern Humans. *Current Anthropology* **39**: S79–S113.
- Marean CW, Spencer LM. 1991. Impact of carnivore ravaging on zooarchaeological measures of element abundance. *American Antiquity* **56**: 645–658.
- Marks AE, Freidel DA. 1977. Prehistoric settlement patterns in the Avdat/Aqev area. In *Prehistory and Paleoenvironments in the Central*

- Negev, Israel. Vol. 2 *The Avdat/Aqev Area, Part 2 and Har Harif*, Marks AE (ed). SMU Press: Dallas; 131–158.
- McCown TD, Keith A. 1939. *The Stone Age of Mt. Carmel II. The Fossil Human Remains from the Levallois-Mousterian*. Clarendon Press: Oxford.
- Mendelssohn H, Yom-Tov Y. 1999. *Fauna Palestina: Mammalia of Israel*. The Israel Academy of Sciences and Humanities: Jerusalem.
- Metcalfe D, Jones KT. 1988. A reconsideration of animal body part utility indices. *American Antiquity* **53**: 486–504.
- Murray AS, Wintle AG. 2000. Luminescence dating of quartz using improved single-aliquot regenerative-dose protocol. *Radiation Measurements* **32**: 57–73.
- Neuvill R. 1951. *Le Paleolithique et le Mesolithique du Desert de Judee*. Masson: Paris.
- Oliver JS. 1989. Analogues and site context: bone damages from Shield Trap Cave (24CB91), Carbon County, Montana, U.S.A. In *Bone Modification*, Bonnicksen R, Sorg MH (eds). University of Maine Center for the Study of First Americans: Orono; 73–98.
- Peleg Y, Marder O, Belmaker M, et al. 2010. Emanuel Cave. *Excavations and Surveys in Israel* 122 (available online at [http://www.hadashot-esi.org.il/report\\_detail\\_eng.asp?id=1589](http://www.hadashot-esi.org.il/report_detail_eng.asp?id=1589)).
- Pickering TR. 2002. Reconsideration of criteria for differentiating faunal assemblages accumulated by hyenas and hominids. *International Journal of Osteoarchaeology* **12**: 127–141.
- Pickering TR, Marean CW, Dominguez-Rodrigo M. 2003. Importance of limb bone shaft fragments in Zooarchaeology: a response to: "On *in situ* attrition and vertebrate body parts profiles" (2002) by M. C. Stiner. *Journal of Archaeological Science* **30**: 1469–1482.
- Porat N. 2007. *Analytical Procedures in the Luminescence Dating Laboratory*. Geological Survey of Israel (2007) Technical Report TR-GSI/2/2007 (in Hebrew).
- Porat N, Rosen SA, Avni Y, et al. 2006. Dating the Ramat Saharonim Late Neolithic Desert Cult Site. *Journal of Archaeological Science* **33**: 1341–1355.
- Rabinovich R. 1990. Taphonomic research of the faunal assemblage from the Quneitra site. In *Quneitra: A Mousterian Site on the Golan Heights*, Goren-Inbar N (ed.). Quedem Monographs of Archaeology: Jerusalem; 189–219.
- Rabinovich R. 2003. The Levantine Upper Palaeolithic faunal record. In *More Than Meets The Eye: Studies on Upper Palaeolithic Diversity in the Near East*, Goring-Morris AN, Belfer-Cohen A (eds). Oxbow: Oxford; 33–48.
- Rabinovich R, Bar-Yosef O, Vandermeersch B, et al. 2004. Hominid–carnivore interactions in the Palaeolithic site of Qafzeh Cave, Israel. *Revue de Paleobiologie, Geneve* **23**: 627–637.
- Rabinovich R, Hovers E. 2004. Faunal analysis from Amud Cave: preliminary results and interpretations. *International Journal of Osteoarchaeology* **14**: 287–306.
- Rabinovich R, Tchernov E. 1995. Chronological palaeological and taphonomical aspects of the Middle Palaeolithic site of Qafzeh, Israel. In *Archaeozoology of the Near East II*, Buitenhuis H, Uerpmann H-P (eds). Backhuys Publishers: Leiden; 5–44.
- Reed DN. 2005. Taphonomic implications of roosting behavior and trophic habits in two species of African owl. *Journal of Archaeological Science* **32**: 1669–1676.
- Saltz D. 1998. A long-term systematic approach to planning reintroductions: the Persian fallow deer and Arabian Oryx in Israel. *Animal Conservation* **1**: 245–252.
- Sass E, Bein A. 1978. Platform carbonates and reefs in the Judean Hills, Carmel and Galilee. *Tenth International Congress on Sedimentology*, Jerusalem, 1978. International Association of Sedimentologists: Jerusalem; 239–274.
- Sharon G, Grosman L, Fluck H, et al. 2010. The first two excavation seasons at NMO: a Mousterian site at the Bank of the Jordan River. *Eurasian Prehistory* **7**: 135–157.
- Sneh A, Bartov Y, Rosenshaft M. 1998. *Geological Map of Israel*, 1:200,000, Sheet 2. Geological Survey of Israel: Jerusalem.
- Speth JD, Tchernov E. 2007. The Middle Palaeolithic occupations at Kebara Cave: a faunal perspective. In *Kebara Cave, Mt. Carmel, Israel. The Middle and Upper Palaeolithic Archaeology*, Part 1, Bar-Yosef O, Meignen L (eds). Peabody Museum of Archaeology and Ethnology: Cambridge; 165–260.
- Steele TE. 2005. Comparing methods for analyzing mortality profiles in zooarchaeological and palaeontological samples. *International Journal of Osteoarchaeology* **15**: 404–420.
- Stiner MC. 1994. *Honor among Thieves: A Zooarchaeological Study of Neandertal Ecology*. Princeton University Press: Princeton.
- Stiner MC. 2002. On *in situ* attrition and vertebrate body part profiles. *Journal of Archaeological Science* **29**: 979–991.
- Stiner MC. 2005. *The faunas of Hayonim Cave (Israel): A 200,000-Year Record of Paleolithic Diet, Demography and Society*. Peabody Museum of Archaeology and Ethnology: Cambridge, MA.
- Stiner MC, Achyuthan H, Arsebuk G, et al. 1998. Reconstructing cave bear paleoecology from skeletons: a cross-disciplinary study of Middle Pleistocene bears from Yarimbuzaz Cave, Turkey. *Paleobiology* **24**: 74–98.
- Stiner MC, Barkai R, Gopher A. 2009. Cooperative hunting and meat sharing 400–200 kya at Qesem Cave, Israel. *Proceedings of the National Academy of Sciences* **106**: 13207–13212.
- Stiner MC, Gopher A, Barkai R. 2011. Hearth-side socioeconomics, hunting and paleoecology during the late Lower Paleolithic at Qesem Cave, Israel. *Journal of Human Evolution* **60**: 213–233.
- Tchernov E. 1992. Biochronology, paleoecology, and dispersal events of hominids in the Southern Levant. In *The Evolution and Dispersal of Modern Humans in Asia*, Akazawa T, Aoki K, Kimura T (eds). Hokusen-Sha: Japan; 149–188.
- Tchernov E. 1998. The faunal sequences of the Southwest Asian Middle Palaeolithic in relation to hominid dispersal events. In *Neandertals and Modern Humans in Western Asia*, Akazawa T, Aoki K, Bar-Yosef O (eds). Plenum Press: New York; 77–90.
- Tchernov E, Tsoukala E. 1997. Middle Pleistocene (Early Toringian) carnivore remains from Northern Israel. *Quaternary Research* **42**: 122–136.
- Torre I, Arrizabalaga A, Flaquer C. 2004. Three methods for assessing richness and composition of small mammal communities. *Journal of Mammalogy* **85**: 524–530.
- Vaks A, Bar-Matthews M, Ayalon A, et al. 2006. Paleoclimate and location of the border between Mediterranean climate region and the Saharo-Arabian desert as revealed by speleothems from the northern Negev Desert, Israel. *Earth and Planetary Science Letters* **249**: 384–399.
- Vaks A, Bar-Matthews M, Ayalon A, et al. 2007. Desert speleothems reveal climatic window for African exodus of early modern humans. *Geology* **35**: 831–834.
- Vandermeersch B. 1981. *Les Hommes Fossiles de Qafzeh, Israel*. CNRS Editions: Paris.
- Villa P, Mahieu E. 1991. Breakage patterns of human long bones. *Journal of Human Evolution* **21**: 27–48.
- Weinstein-Evron M, Bar-Oz G, Zaidner Y, et al. 2003. Introducing Misliya Cave: a new continuous Lower/Middle Palaeolithic sequence in the Levant. *Eurasian Prehistory* **1**: 31–55.
- Yeshurun R. 2010. *Middle Paleolithic prey-choice patterns as revealed from a natural pitfall trap: Rantisi Cave, Israel*. Poster presented at the ICAZ meeting, August 2010, Paris, France.
- Yeshurun R, Bar-Oz G, Weinstein-Evron M. 2007. Modern hunting behavior in the early Middle Paleolithic: faunal remains from Misliya Cave, Mount Carmel, Israel. *Journal of Human Evolution* **53**: 656–677.
- Yom-Tov Y, Wool D. 1997. Do the contents of barn owl pellets accurately represent the proportion of prey species in the field? *The Condor* **99**: 972–976.